A High-Resolution Interpolation at Arbitrary Interfaces for the FDTD Method

Jacek Nadobny, Dennis Sullivan, *Senior Member, IEEE*, Peter Wust, Martin Seebass, Peter Deuflhard, and Roland Felix

***Abstract*— In recent years, the finite-difference time-domain (FDTD) method has found numerous applications in the field of computational electromagnetics. One of the strengths of the method is the fact that no elaborate grid generation specifying the content of the problem is necessary—the medium is specified by assigning parameters to the regularly spaced cubes. However, this can be a weakness, especially when the interfaces between neighboring media are curved or "sloped" and do not exactly fit the cubic lattice. Since the E- and H-fields are only calculated at the regular intervals, sharp field discontinuities at the interfaces are often missed. Furthermore, the averaging of the material properties often leads to significant errors. In this paper, a post-processing method is presented, which approximates the correct field behavior at the interfaces by interpolating between the FDTD calculated values, splitting them into the components normal and tangential to the interfaces, and then enforcing the interface conditions for each of these components separately.**

***Index Terms*—Averaging of material properties, biological media, curved and "sloped" interfaces, FDTD method, flux-related fields, interface conditions, layered spheres, linear interpolations, Mie series solutions.**

I. Introduction

ONE OF THE most widely used methods in computational electromagnetics is the finite-difference time-domain (FDTD) method [1]–[4]. This method is a straightforward implementation of the time-domain Maxwell's equations into a finite-differencing scheme. The strength of the method is its simplicity, lending it to easy implementation into a broad range of applications.

An important characteristics of the FDTD method is the fact that it does not require the generation of a complicated grid to define the problem domain as is often used, for instance, in the finite-element method [5] or the volume surface integral-equation method [6], [7]. The FDTD problem domain is usually made up of cubes, and the material parameters are assigned to these cubes. This, of course, may also be a weakness, limiting the accuracy to which any surface can be defined according to the "stair casing" of the FDTD formulation. Furthermore, the averaging of the material properties at interfaces between neighboring media often leads to significant errors. The reasons for these problems are inherent to the FDTD method: firstly, the field components are only calculated at uniform spatially shifted intervals, and secondly, and more importantly, the FDTD method calculates E-field (and H-field) components *indirectly* from electric (and magnetic) fluxes, which cross perpendicular quadratic surfaces constructed by the H-lines (and E-lines) associated with curl-related line integrals over H (and E) [8]. The relationship between the field components and the flux values is not trivial if the interfaces are curved or "sloped" and/or do not exactly fit the cubic lattice. Problems of the discontinuity of fields have to be taken into account—especially for such interfaces.

There have been hybrid FDTD formulations that used more complex structures [8]–[12] than simple cubes. However, deviations from the regular grid formulation always present more complications and time spent in generating the problem domain.

In this paper, we present a formulation for postprocessing of the FDTD simulation that can significantly improve the resolution of the FDTD at interfaces. This formulation uses the fields calculated by a standard FDTD program, then interpolates at points between the FDTD calculated values, and then "corrects" the interpolated results in the frequency domain based on the geometry of interfaces and parameters of the surrounding medium. Since it is only done once, upon completion of an FDTD simulation, it does not substantially add to the simulation time. We present a formulation for electrically inhomogeneous and magnetically homogeneous media ("biological" media), although a similar formulation can be derived for magnetically inhomogeneous media. An explanation of the formulation will be presented, followed by examples of FDTD calculations, which are verified by analytic results based on Bessel-function expansions. It will also be shown that this "corrector" can correct significant errors that the FDTD had made at interfaces.

II. Formulation

We begin with a general overview of the idea. Fig. 1 shows an interface dividing two regions, one consisting of a material with a permittivity ε_1, the other with ε_2. $\mathbf{E}$ is the exact E-field

Manuscript received November 15, 1996; revised June 8, 1998. This work was supported by Berliner Sparkassenstiftung Medizin, Deutsche Krebshilfe e.V., and by Deutsche Forschungsgemeinschaft (Sonderforschungsbereich 273).

J. Nadobny is with the Clinic for Radiation Medicine, Charité–Campus Virchow-Klinikum, Medical School of Humboldt University at Berlin, 13353 Berlin, Germany (e-mail: nadobny@zib.de), and also with Konrad–Zuse–Zentrum fuer Informationstechnik Berlin (ZIB), D-14195 Berlin, Germany.

D. Sullivan is with the Department of Electrical Engineering, University of Idaho, Moscow, ID 83844-1023 USA.

P. Wust and R. Felix are with the Clinic for Radiation Medicine, Charité–Campus Virchow-Klinikum, Medical School of Humboldt University at Berlin, 13353 Berlin, Germany.

M. Seebass and P. Deuflhard are with Konrad–Zuse–Zentrum fuer Informationstechnik Berlin (ZIB), D-14195 Berlin, Germany.

Publisher Item Identifier S 0018-9480(98)08115-0.

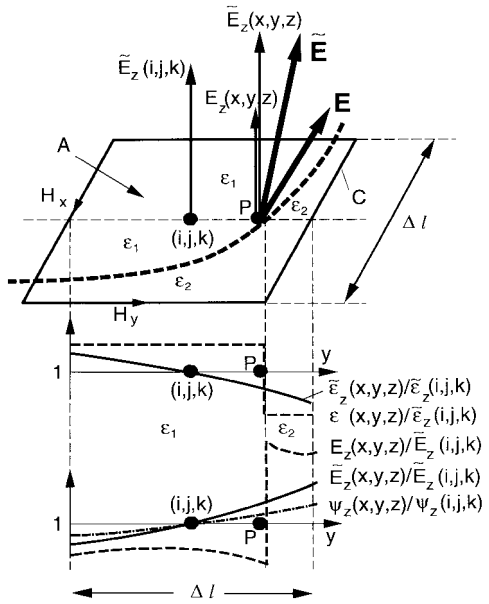

Fig. 1. Fields within the contour of a "H-loop-surface" A in the Yee cell in close proximity to an interface given by the permittivity values ε_1 and ε_2. The relationship between the "exact" values [$E_z(x, y, z)$, $\varepsilon(x, y, z)$, ε_z is either ε_1 or ε_2], the averaged, "flux related," FDTD values ($\tilde{E}_z(x, y, z)$, $\tilde{\varepsilon}_z(x, y, z)$), and the flux $\Psi_z(x, y, z)$ through surface A due to the translation of A (and the entire FDTD lattice) in the y-direction in relation to a fixed position of the interface between ε_1 and ε_2. The approximation of this translation effect for averaged values (linear interpolation) is described in the Appendix. The "recovery" scheme of the "exact" solution from averaged values is given by (12).

in the medium ε_1 at a location next to the interface (point P in Fig. 1), $\tilde{\mathbf{E}}$ is an averaged value that has been obtained by the standard FDTD method. (An analogous procedure can be applied with a different value of $\mathbf{E}$ to medium ε_2 at the other side of the interface, which, for simplicity, is not shown.) The statement of the problem is: $\tilde{\mathbf{E}}$ is what we have, but $\mathbf{E}$ is what we want. To put the problem in the perspective of the FDTD formulation, Fig. 1 illustrates the calculation (Ampere's law) of the z-component of the electric field via electric flux Ψ_z through the surface A bounded by a contour C as follows:

$$\frac{\partial}{\partial t}\Psi_z = \oint_C \mathbf{H} \bullet \mathbf{dl} \tag{1a}$$

where the relationship between Ψ_z and the exact field distribution $E_z(x, y, z)$ on A is given by

$$\Psi_z = \int\int_A \varepsilon \mathbf{E} \bullet \mathbf{dA} = \int\int_A \varepsilon(x, y, z) E_z(x, y, z) dx\, dy \tag{1b}$$

where $A = \Delta l^* \Delta l$, Δl is the length of the cube's edge. The surface A crosses an interface between ε_1 and ε_2 such that one part of A belongs to medium ε_1, and the other part to medium ε_2, respectively. Thus, for this case, $\varepsilon(x, y, z)$ in (1b) is either ε_1 or ε_2. The standard FDTD methodology is to discretize (1a) using the spatial differencing of the surrounding H_y and H_x values in order to calculate the new value of flux Ψ_z through A at the time step n at the point in the FDTD lattice specified by (i, j, k), defined in the center of the "H-loop-surface" A as follows:

$$\begin{aligned}\Psi_z^n(i, j, k) &\cong \Psi_z^{n-1}(i, j, k) + \Delta T \cdot \Delta l \\ &\cdot \Big(H_x^{n-(1/2)}\big(i, j - \tfrac{1}{2}, k\big) - H_x^{n-(1/2)}\big(i, j + \tfrac{1}{2}, k\big) \\ &+ H_y^{n-(1/2)}\big(i + \tfrac{1}{2}, j, k\big) - H_y^{n-(1/2)}\big(i - \tfrac{1}{2}, j, k\big) \Big).\end{aligned} \tag{2a}$$

From this, an averaged, ("flux-related") FDTD value of the electric field at the time step n is obtained via a simple approximation of (1b) as follows:

$$\tilde{E}_z^n(i, j, k) \approx \frac{\Psi_z^n(i, j, k)}{\tilde{\varepsilon}_z(i, j, k) \cdot \mathrm{A}} \tag{2b}$$

where the averaged dielectric constant throughout the H-loop-surface A in (2b) is given by

$$\tilde{\varepsilon}_z(i, j, k) = \frac{1}{\mathrm{A}} \cdot \int\int_{\mathrm{A}} \varepsilon(x, y, z) \cdot dx\, dy. \tag{3}$$

In general, $\varepsilon(x, y, z)$ in (1b) can represent a real dielectric constant and a conductivity. Thus, in the frequency domain, it will be complex. Thus, for the disretization of (1b), an additional averaging over conductivity values is necessary (not shown here).

As a result of an FDTD run, we obtain (in the frequency domain) a set of values in the lattice points, either $\Psi_z(i, j, k)$ or $\tilde{E}_z(i, j, k)$. [Only one set must be stored, another one is directly given via (2b), which is also valid in the frequency domain for complex $\tilde{\varepsilon}_z(i, j, k)$.] Theoretically, in order to obtain $\tilde{E}_z$ or Ψ_z *between* the lattice points, we could translate the FDTD lattice with respect to a fixed geometry and run the FDTD calculation again. Repeating this numerous times, and defining for each FDTD run $P(x, y, z)$ as the new position of the "old" lattice point (i, j, k), we would obtain a set of values $\Psi_z(x, y, z)$, $\tilde{\varepsilon}_z(x, y, z)$, and $\tilde{E}_z(x, y, z)$, as indicated in Fig. 1. [In the practical implementation, the effect of this translation will be approximated by an interpolation (see Appendix).] In general, due to the averaging of (2a) and (3), the averaged distribution $\tilde{E}_z$ would be *continuous* with respect to the translation in the x- and y-directions, i.e., continuous on the "old" H-loop-surface A, independent of the geometry of the interface. In contrast, the "exact" distribution E_z is usually *discontinuous* on A, it "jumps" during transitions between the media ε_1 and ε_2. Thus, in order to take this discontinuity into account, the averaged distribution $\tilde{E}_z$ must, in most cases, be *corrected*, with the exception of two special cases: the trivial case of a homogeneous cell $\tilde{\varepsilon}_z = \varepsilon_1 = \varepsilon_2$ and the case of the interface normal being perpendicular to the z-direction. In the latter case, $E_z(x, y, z)$ is also continuous on A and, therefore, can be represented by $\tilde{E}_z(x, y, z)$. Notice that for the limit case of a constant value of E_z on A, the remaining integration in (1b) becomes identical with the integration in (3). Thus, (2b) implicitly yields the exact value $\tilde{E}_z = Ez$.

Referring again to Figs. 1 and 2, both the "exact" and the averaged E-field vectors can be described by the sum of the

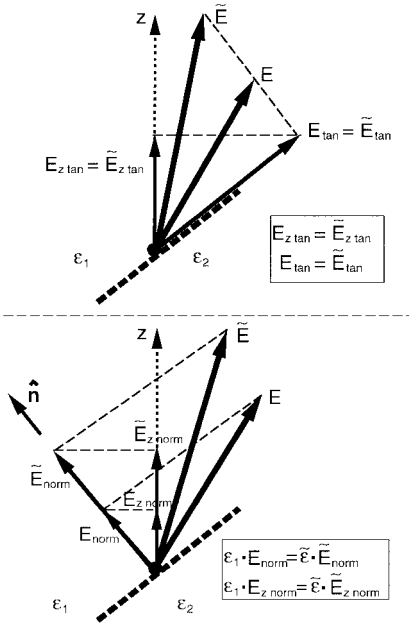

Fig. 2. Splitting of the "exact" ($\mathbf{E}$) and averaged ($\tilde{\mathbf{E}}$) FDTD fields into the tangential (above) and normal (below) directions with respect to the interface between ε_1 and ε_2, and subsequent projection into the z-direction.

components tangential and normal to the nearby interface [the coordinate index x, y, z is left out for simplicity for all expressions in (4)–(11)]

$$\mathbf{E} = \mathbf{E}_{\tan} + \mathbf{E}_{\text{norm}} \tag{4}$$

$$\tilde{\mathbf{E}} = \tilde{\mathbf{E}}_{\tan} + \tilde{\mathbf{E}}_{\text{norm}}. \tag{5}$$

At this point, according to the above discussion of the standard FDTD discretization, we make two key assumptions: 1) The tangential component of the averaged FDTD value is equal to the tangential component of the "exact" value of E ($\mathbf{E}_{\tan} \cong \tilde{\mathbf{E}}_{\tan}$, shown in Fig. 2). Consequently, also for their z-components,

$$E_{z\tan} \cong \tilde{E}_{z\tan}. \tag{6}$$

2) The normal component of the flux density is a constant throughout the interface between ε_1 and ε_2 for "exact" and averaged distributions (see Fig. 2). Therefore, in medium ε_1 for the z-components

$$\varepsilon_1 \cdot E_{z\,\text{norm}} \cong \tilde{\varepsilon}_z \cdot \tilde{E}_{z\,\text{norm}}. \tag{7}$$

The relationships in (4) and (5) can be interpreted as the three separate equations corresponding to the three directions, one set of which is

$$E_z = E_{z\tan} + E_{z\,\text{norm}} \tag{8}$$

$$\tilde{E}_z = \tilde{E}_{z\tan} + \tilde{E}_{z\,\text{norm}}. \tag{9}$$

Substituting (6) and (9) into (8), gives

$$E_z \cong \tilde{E}_z - \tilde{E}_{z\,\text{norm}} + E_{z\,\text{norm}}. \tag{10}$$

Finally, using (7), we get

$$E_z \cong \tilde{E}_z + \left(\frac{\tilde{\varepsilon}_z}{\varepsilon_1} - 1\right) \cdot \tilde{E}_{z\,\text{norm}} \tag{11}$$

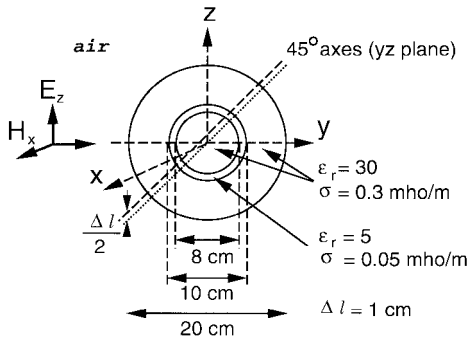

Fig. 3. Test configuration used to evaluate the FDTD results via Bessel-function expansion. The "45° axes" in the YZ-plane. Notice that due to the specification of the Yee cells (1-cm size) with respect to the geometry of the sphere, the lattice points for E_z- and for E_y-FDTD computation are located on the 45° axis, indicated as a dashed line, which is shifted a half-cell length (0.5 cm) in the z-direction with respect to the "exact 45° axis" (dotted line).

or, more generally, for all points in the FDTD domain,

$$E_z(x, y, z) \cong \tilde{E}_z(x, y, z) + \left(\frac{\tilde{\varepsilon}_z(x, y, z)}{\varepsilon(x, y, z)} - 1\right) \cdot \tilde{E}_{z\,\text{norm}}(x, y, z). \tag{12}$$

Equation (12) is the heart of the method. The second term on the right is the "correction," i.e., the difference between the averaged FDTD value and the "exact" value. $\tilde{E}_{z\,\text{norm}}$ in (12) is calculated from the scalar product of the averaged FDTD vector $\tilde{\mathbf{E}}$ and the unit normal vector at the interface $\hat{\mathbf{n}}$

$$\tilde{E}_{z\,\text{norm}}(x, y, z) = \hat{n}_z(x, y, z) \cdot \{\hat{\mathbf{n}}(x, y, z) \bullet \tilde{\mathbf{E}}(x, y, z)\}. \tag{13}$$

$\hat{n}_z$ is the z-component of $\hat{\mathbf{n}}$. $\hat{\mathbf{n}}$ is derived from the gradient of $\tilde{\varepsilon}$ (see Appendix), i.e., $\hat{\mathbf{n}}$ [and, consequently, also $\tilde{E}_{z\,\text{norm}}$ in (13)] are nonzero, not only directly at the interface, but also for other points on the H-loop-surface A, where the correction (12) is necessary. Analogous expressions to (12) and (13) can be derived for x- and y-directions using $\tilde{E}_{x/y}$, $\tilde{\varepsilon}_{x/y}$, $\tilde{E}_{x/y\,\text{norm}}$, and $\hat{n}_{x/y}$, respectively.

A. Remarks

1) If the cell is homogeneous (the case $\tilde{\varepsilon} = \varepsilon$ on A), the second term in (12) goes to zero. Similarly, if the interface normal $\hat{\mathbf{n}}$ is perpendicular to the z-direction, then $\tilde{E}_{z\,\text{norm}} = 0$ and, again, the second term in (12) goes to zero. Either of these two situations result in the uncorrected FDTD value being equal to the "exact" value.
2) It can be shown that applying (12) to a pair of points which are situated on different sides of the interface in the media ε_1 and ε_2, respectively, the continuity of the normal flux density is implicitly enforced via (12). [Notice that for such points, the right side of (11) is identical, except from $\varepsilon_{1/2}$.]
3) In (12), ε is used as the exact value of the dielectric constant at the point where the calculation was made. It is the relationship between this value and $\tilde{\varepsilon}$, the averaged value that the FDTD program uses, which is an inherent part of the correction. However, the concept

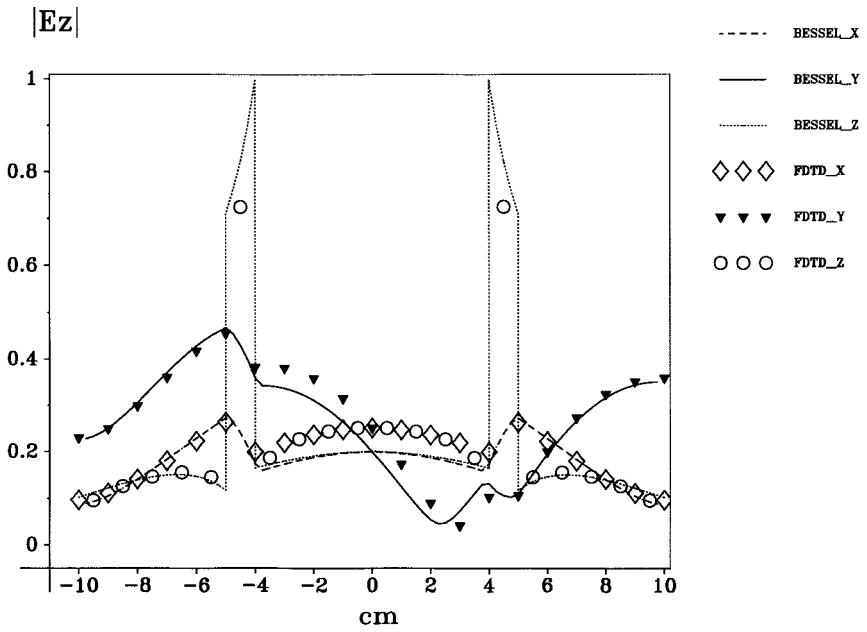

Fig. 4. Comparison of FDTD versus Bessel-function expansion at 300 MHz along the three principal axes x, y, z using the lossy dielectric sphere described in Fig. 3.

of an "exact" ε must often be taken with a grain of salt. It could simply be that the medium is known to somewhat better precision than the resolution used in the FDTD computation. For instance, it could be that the medium is divided into small 1-mm^3 cubes, but computational restrictions dictate that only big 1-cm^3 cells can be used in the FDTD formulation. Therefore, the $\tilde{\varepsilon}$ values would be obtained by averaging small cells through out the H-loop-surfaces. Or, more specifically, in hyperthermia cancer-therapy simulation, the courser FDTD parameters are derived from the finer pixel values of computer tomography (CT) scans [13].

III. Procedure

The following list describes the implementation of the correcting procedure step-by-step.

1) The "exact" geometry $\varepsilon(x, y, z)$ is defined. The position and size of Yee cells (i, j, k) and, therefore, the positions (i, j, k) of three E-field and three H-field components are specified with respect to $\varepsilon(x, y, z)$. For each of the three E-field components $\nu, \nu = x, y, z$ averaged permittivity values $\tilde{\varepsilon}_\nu(i, j, k)$ are calculated and stored (3).
2) The FDTD method is run, resulting in the calculation of $\Psi_\nu(i, j, k)$ for each of the three directions $\nu, \nu = x, y, z$ (2a).
3) A set of arbitrarily located points (x, y, z), in which the "exact" solution should be calculated, is defined in the medium $\varepsilon(x, y, z)$.
4) The interpolated values of $\tilde{\varepsilon}_\nu(x, y, z)$, and $\Psi_\nu(x, y, z)$ are calculated at these points using the interpolation in (A1). From these, $\tilde{E}_\nu(x, y, z)$ values are calculated via (A3).
5) The interface unit normal $\hat{\mathbf{n}}(x, y, z)$ is calculated from (A4a) via (A4b) using the permittivity gradients. Finally, the normal components $\tilde{E}_{\nu\,\mathrm{norm}}(x, y, z)$ are obtained using (13).
6) Now all necessary parameters are available, and for each component $\nu, \nu = x, y, z$, the corrected values $E_\nu(x, y, z)$ are calculated by (12), resulting in the "exact" vector $\mathbf{E}(x, y, z)$.

IV. Evaluation

Fig. 3 illustrates a test problem, which can be used to demonstrate the effectiveness of this method. By using layered spheres illuminated by plane wave at 300 MHz, a comparison can be made between FDTD calculated values and those calculated by Bessel-function expansions [14]. The E-field vectors of the plane wave are polarized in the z-direction, and the wave is propagating in y-direction. The sphere is 20 cm in diameter and consists mostly of a material with dielectric constant $\varepsilon_r = 30$ and conductivity of $\sigma = 0.3$ mho/m. This is chosen to be representative of biological tissues, which range somewhere between $\varepsilon_r = 70$, $\sigma = 0.9$ mho/m for high-water-content tissues like muscle, and $\varepsilon_r = 5$, $\sigma = 0.05$ mho/m for low-water-content tissues like bone or fat. Between 4- and 5-cm radii is a 1-cm-thick strip of fat- or bone-like tissue at $\varepsilon_r = 5$, $\sigma = 0.05$ mho/m. This is typical of a biological medium where a small strip of bone or fat causes a sharp discontinuity that is often difficult for an FDTD method to account for. Fig. 4 shows a comparison between the analytic values with those from an FDTD calculation along the principal axes using 1-cm cells. The z-component of the E-field is compared here. At this point, it is important to discuss the chosen position of the E-field components in the FDTD lattice with respect to the sphere's geometry. The center of the sphere [point (0, 0, 0)] matches the center of the Yee cell, i.e., E-fields are offset one-half-cell length in their own direction with respect to the sphere's center. Thus, H-loop-surfaces associated with E_z-lattice points on the axis z [e.g., points (0,

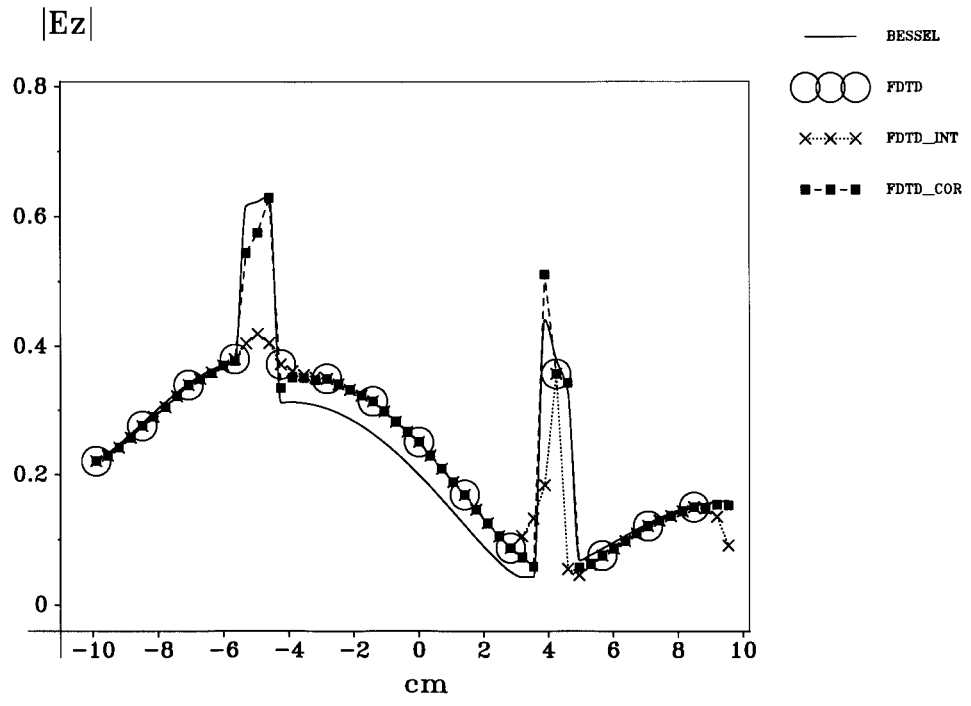

(a)

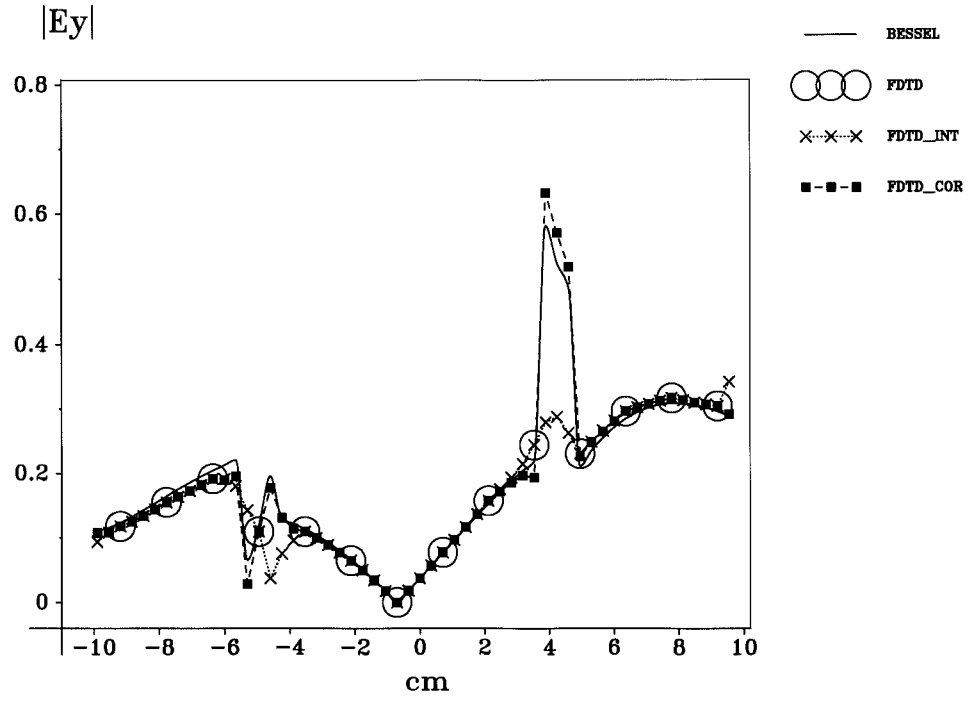

(b)

Fig. 5. (a) Comparison of FDTD values in lattice points ("FDTD"), FDTD values linearly interpolated at 0.25-cm intervals without ("FDTD_INT") and with ("FDTD_COR") the corrector (12) versus theoretical values ("BESSEL") of the z-component of the E-field on the 45° axis, indicated as the dashed line in Fig. 3. The zero abscissa value is at the E_z-lattice point (0, 0, +0.5). The "FDTD_COR"-solution "removes" the smoothing effect of the "FDTD-INT"-interpolation and "recovers" the field discontinuities in the "fat" layer. (b) Comparison as in (a) for the y component of the E-field. Again, the "FDTD_COR"-solution matches the analytical solution best.

0, 4.5), (0, 0, 5.5), etc.] lie in a single medium, corresponding to the homogeneous case $\tilde{\varepsilon} = \varepsilon$ with zero correction in (12). [Indeed, the FDTD results on this axis are good (see Fig. 4); the high E_z-value in the "fat" layer is reproduced, which is in accordance with the discussion in Section II, concluding that no correction is necessary for homogeneous cells.] On the other hand, for axes x and y, there are E_z-lattice points, which are located in the vicinity of interfaces, where corresponding H-loop-surfaces are intersected by two media [e.g., points (0, 4, 0.5) or (0, 5, 0.5), etc.]. However, as the interface normal in these points is almost perpendicular to z, i.e., almost "nonsloped," no E_z-"jumps" occur there, and the correction

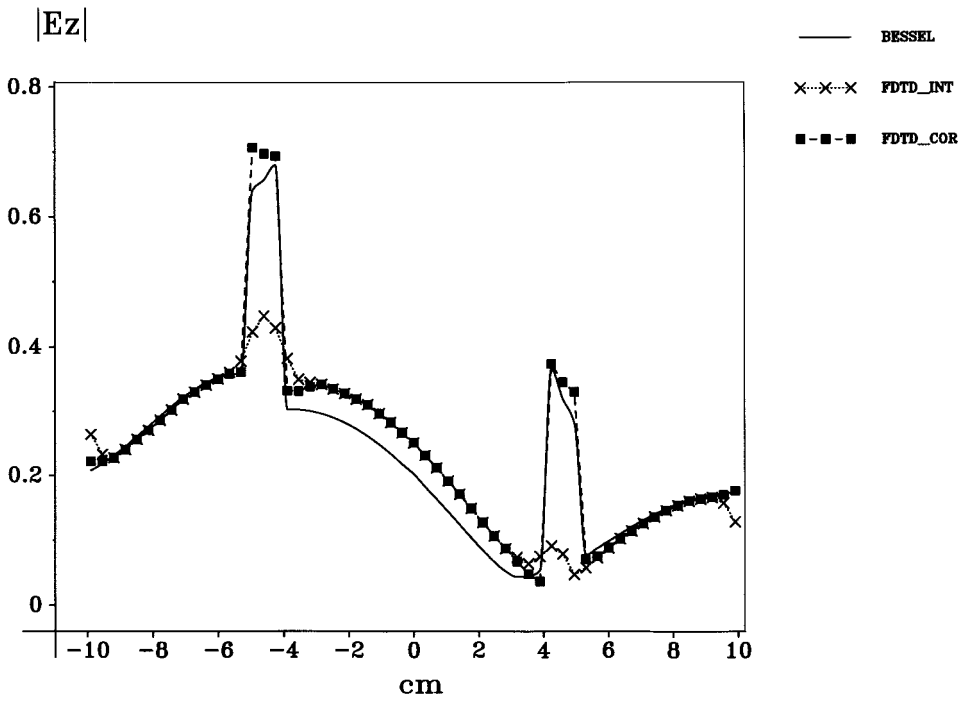

Fig. 6. Comparison of FDTD values linearly interpolated at 0.25-cm intervals without ("FDTD_INT") and with ("FDTD_COR") the corrector (12) versus theoretical values ("BESSEL") of the z-component of the E-field on the "exact 45° axis," indicated as the dotted line in Fig. 3. The zero abscissa value is at the central sphere point (0, 0, 0). Also in this case, the "FDTD_COR"-values reproduce field discontinuities correctly.

(12) is again zero. [Indeed, the FDTD results are also good for these axes (see Fig. 4), which is again in accordance with the discussion in Section II, concluding that no correction is necessary for nonsloped interfaces.] As a conclusion for Fig. 4, the chosen FDTD lattice resolution of 1 cm, i.e., in the range of the fat layer, yields satisfactory results along the principal axes. However, problems come outside the symmetry axes where the interfaces can be "sloped" with respect to the Cartesian-field components, i.e., where the FDTD results should be corrected. Fig. 5(a) and (b) refers to the position of the sloped "45° axis," which is indicated in Fig. 3 as a dashed line. As this axis is shifted 0.5 cm in the positive z-direction—it meets exactly several lattice points for E_z and for E_y computation in the sphere [values "FDTD" in Fig. 5(a) and (b)]. Thus, the effects of a poor resolution of the FDTD solution can be directly studied along this axis. For example, the FDTD calculation of E_z [see Fig. 5(a)] around -4.5 cm (and analogously of E_y [see Fig. 5(b)] around $+4.5$ cm) did not have a lattice point in the fat layer, and the sharp discontinuities were missed there. It did catch the E_z-peak [see Fig. 5(a)] around 4.5 cm (and it calculated the correct E_y-value [see Fig. 5(b)] around -4.5 cm) because it had a lattice point for E_z (and E_y) in the fat layer.

To illustrate the improvement of the resolution at this axis using the postprocessing routine, two other sets of values derived from the FDTD program are plotted in Fig. 5(a) and (b). The first are values of the z-component [see Fig. 5(a)] and of the y-component [see Fig. 5(b)] of the E-field at 0.25-cm intervals ("FDTD_INT"), calculated via interpolation (A3) without the corrector (12). This simple interpolation did little to alleviate the missed $E_{z/y}$-peaks around ± 4.5 cm [see Fig. 5(a) and (b)], it performed an averaging at interfaces around the E_z-peak at 4.5 cm [see Fig. 5(a)], and it calculated a wrong field gradient around the E_y value at -4.5 cm in the fat layer [see Fig. 5(b)].

The second set of values ("FDTD_COR") is obtained using the corrector (12) in combination with the interpolation scheme (A3). Clearly, this is a superior calculation. The field discontinuities at the interfaces are correctly reproduced. The FDTD-inherent averaging at interfaces is "removed." Even the complicated behavior of the E_y-component in the fat layer around -4.5 cm [see Fig. 5(b)] is well approximated.

The corrector (12) is improving the solution also on axes, which do not meet any FDTD-lattice points (in Fig. 6, the "exact 45° axis," indicated in Fig. 3 as a dotted line, only the E_z-component is shown). Thus, only interpolated FDTD results can be compared on this axis, and the effects of the poor resolution of the FDTD solution are even more evident than in Fig. 5(a). Without the corrector (12), even both peaks, at ± 4.5 cm are missed (curve "FDTD_INT"). In contrast, applying the corrector (12), the field behavior at the interfaces is reproduced correctly ("FDTD_COR").

The correction procedure can be also applied to layers, which are much thinner than the separation of the calculation points in the FDTD lattice (see Fig. 7). In this figure, a similar problem as in Fig. 6 is investigated using a 0.25-cm fat layer centered at the 5-cm radius. The FDTD program is still using 1-cm cells. Once again, a simple interpolation ("FDTD_INT") on the "exact 45° axis" could not "see" any peaks in the fat layer (not shown). However, the "corrected" solution ("FDTD_COR") recognizes the peaks, for both, z- and y-components, even though it does not get the values exactly. If we reduced the fat layer to 1/8 cm, we would risk missing the peak if an interpolated value did not occur there. This illustrates the rule of thumb: the interpolated values must have

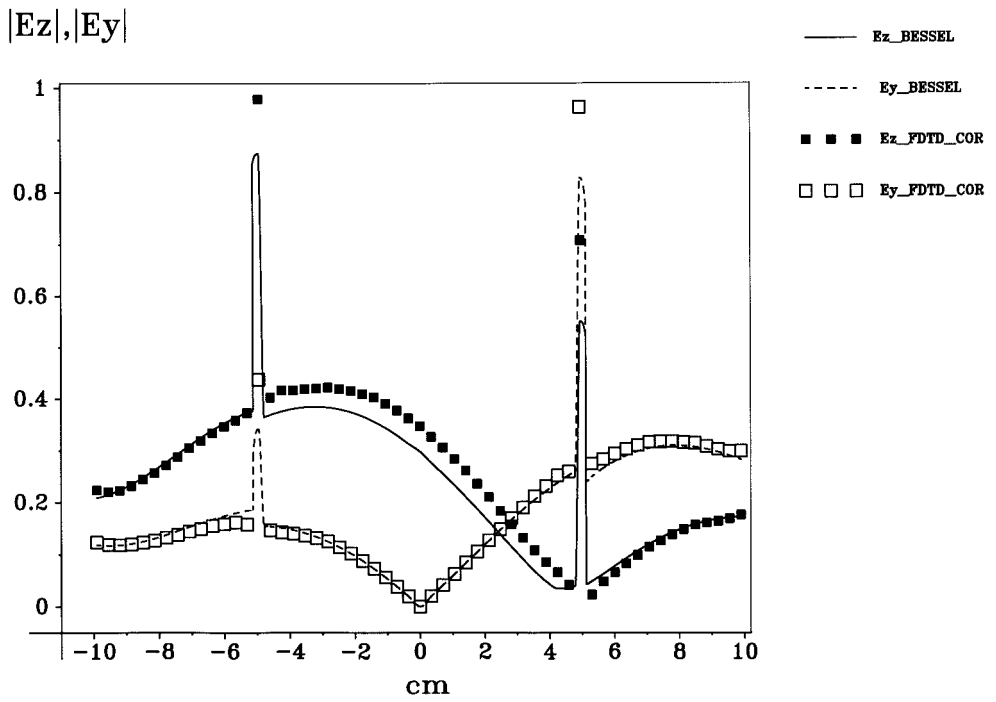

Fig. 7. Comparison of a 1-cm^3 FDTD ("FDTD_COR"-curves) using the corrector (12) versus Bessel-function expansion at 300 MHz along the "exact 45° axis" using a lossy dielectric sphere with a 0.25-cm fat layer centered at the 5-cm radius for both components E_z and E_y. In this small layer, the peaks are reproduced, even though their magnitude is overestimated.

the same resolution as the medium. Of course, the resolution problems of the standard FDTD method can be alternatively reduced applying a finer lattice (not shown). However, apart from higher computation cost, there will always be critical lattice points lying in the vicinity of sloped interfaces where errors may occur.

V. Conclusions

We have presented a procedure which can substantially increase the resolution of an FDTD-based simulation. This is done by interpolating the FDTD calculated values of the E-fields, and then enforcing the discontinuity of the normal component of the interpolated values across boundaries of the media. Since this interpolation is only done after the FDTD simulation is complete, it adds almost nothing to the run time. Comparisons with analytic results from Bessel-function expansions verify the accuracy of the results. This correction procedure might be of a particular importance for algorithms applied to hyperthermia planning systems. It has been shown that results and their clinical interpretations critically depend on the geometry of tissue interfaces [15].

Appendix

Point $P(x, y, z)$ where the averaged ("flux-related") FDTD values are to be interpolated (see also Fig. 1) is situated inside a cubic segment containing eight vertices of the FDTD lattice $(\alpha,\ \beta,\ \gamma)$; $\alpha = i,\ i+1,\ \beta = j,\ j+1,\ \gamma = k, k+1$. [In general, for a single point $P(x,\ y,\ z)$, the combination of vertex numbers $(\alpha,\ \beta,\ \gamma)$ can be different for each of the components of the electric field $\nu,\ \nu = x,\ y,\ z$, which are offset one-half-cell length $(\Delta l/2)$ with respect to each other.] The averaged permittivity $\tilde{\varepsilon}_\nu(x, y, z)$, and the electric flux $\Psi_\nu(x, y, z)$, are interpolated in the frequency domain for each direction $\nu,\ \nu = x,\ y,\ z$ as

$$f_\nu(x, y, z) = \sum_{\gamma=k,\,k+1} \left\{ \sum_{\beta=j,\,j+1} \left(\sum_{\alpha=i,\,i+1} \eta(x, y, z) \cdot f_\nu(\alpha, \beta, \gamma) \right) \right\} \tag{A-1}$$

where $f_\nu(\alpha, \beta, \gamma)$ represents $\tilde{\varepsilon}_\nu(\alpha, \beta, \gamma)$ or $\Psi_\nu(\alpha, \beta, \gamma)$, respectively, which have been calculated by the FDTD method at eight vertices of the cubic FDTD lattice segment. $\eta(x, y, z)$ are the cubic shape functions [5] given by

$$\eta(x, y, z) = (1-|\alpha-x|)\cdot(1-|\beta-y|)\cdot(1-|\gamma-z|). \tag{A-2}$$

The value of the averaged E-field component $\nu,\ \nu = x,\ y,\ z$ in $P(x, y, z)$, which is necessary for the correction (12), is calculated analogously to (2b)

$$\tilde{E}_\nu(x, y, z) \approx (\Psi_\nu(x, y, z))/(\tilde{\varepsilon}_\nu(x, y, z) \cdot \mathrm{A}) \tag{A-3}$$

where $\Psi_\nu(x, y, z)$ and $\tilde{\varepsilon}_\nu(x, y, z)$ are interpolated as in (A1). The interface unit normal vector $\hat{\mathbf{n}}$, which is used in (13), is calculated from

$$\begin{aligned} \hat{\mathbf{n}}(x, y, z) &= (\hat{n}_x, \hat{n}_y, \hat{n}_z) \\ &= (\overline{n}_x, \overline{n}_y, \overline{n}_z)/|(\overline{n}_x, \overline{n}_y, \overline{n}_z)| \end{aligned} \tag{A-4a}$$

where $\overline{n}_\nu = \overline{n}_\nu(x, y, z),\ \nu = x, y, z$ are components of the permittivity gradient. $\overline{n}_\nu(x, y, z)$ is calculated from the interpolated (complex) permittivity values

$$\begin{aligned} \overline{n}_x(x, y, z) &= |\tilde{\varepsilon}_x(x+\delta x, y, z)| - |\tilde{\varepsilon}_x(x-\delta x, y, z)| \\ \overline{n}_y(x, y, z) &= |\tilde{\varepsilon}_y(x, y+\delta y, z)| - |\tilde{\varepsilon}_y(x, y-\delta y, z)| \\ \overline{n}_z(x, y, z) &= |\tilde{\varepsilon}_z(x, y, z+\delta z)| - |\tilde{\varepsilon}_z(x, y, z-\delta z)| \end{aligned} \tag{A-4b}$$

where, for cubic elements, $\delta x = \delta y = \delta z = \Delta l/2$. Notice that all interpolated values have an integral (averaged) sense and describe not only the point $P(x, y, z)$, but also its surrounding in the range of $\pm\Delta l/2$.

REFERENCES

[1] K. S. Yee, "Numerical solution of initial boundary value problems involving Maxwell's equations in isotropic media," *IEEE Trans. Antennas Propagat.*, vol. AP-17, pp. 585–589, 1966.

[2] A. Taflove, "Review of the formulation and applications of the finite-difference time-domain method for numerical modeling of electromagnetic wave interactions with arbitrary structures," *Wave Motion*, vol. 10, pp. 547–582, Dec. 1988.

[3] K. Kunz and R. Luebbers, *The Finite Difference Time Domain Method for Electromagnetics.* Boca Raton, FL: CRC Press, 1993.

[4] K. L Shlager and J. B. Schneider, "A selective survey of the finite-difference time-domain literature," *IEEE Antennas Propagat. Mag.*, vol. 37, pp. 39–56, Aug. 1995.

[5] R. K. Livesley, *Finite Elements: An Introduction for Engineers.* Cambridge, U.K.: Cambridge Univ. Press, 1983.

[6] P. Wust, J. Nadobny, M. Seebass, J. M. Dohlus, W. John, and R. Felix, "3-D computation of the E-fields by the volume-surface integral equation (VSIE) method in comparison with the finite-integration theory (FIT) method," *IEEE Trans. Biomed, Eng.*, vol. 40, pp. 745–759, Aug. 1993.

[7] J. Nadobny, P. Wust, M. Seebass, P. Deuflhard, and R. Felix, "A volume-surface integral equation method for solving Maxwell's equations in electrically inhomogeneous media using tetrahedral grids," *IEEE Trans. Microwave Theory Tech.*, vol. 44, pp. 543–554, Apr. 1996.

[8] K. R. Umashankar and A. Taflove, "Calculation and experimental validation of induced currents on coupled wires in an arbitrary shaped cavity," *IEEE Trans. Antennas Propagat.*, vol. AP-35, pp. 1248–1257, Nov. 1987.

[9] A. Taflove, K. R. Umashankar, B. Bekker, F. Harfoush, and K. S. Yee, "Detailed FD-TD analysis of electromagnetic field penetrating narrow slots and lapped joints in thick conducting screens," *IEEE Trans. Antennas Propagat.*, vol. 26, pp. 247–257, Feb. 1988.

[10] M. Fusco, "FDTD algorithm in curvilinear coordinates," *IEEE Trans. Antennas Propagat.*, vol. 38, pp. 76–89, Jan. 1990.

[11] T. G. Jurgens, A. Taflove, K. Umashankar, and T. G. Moore, "Finite-difference time-domain modeling of curved surfaces," *IEEE Trans. Antennas Propagat.*, vol. 40, pp. 357–366, Apr. 1992.

[12] N. K. Madsen, "Divergence preserving discrete surface integral methods for Maxwell's curl equations using nonorthogonal unstructured grids," *J. Comput. Phys.*, vol. 119, pp. 34–35, 1994.

[13] B. J. James and D. M. Sullivan, "Direct use of CT scans for hyperthermia treatment planning," *IEEE Trans. Biomed. Eng.*, vol. 39, pp. 845–851, 1992.

[14] J. R. Mautz, "Mie series solution for a sphere," *IEEE Trans. Microwave Theory Tech.*, vol. MTT-26, pp. 375–380, May 1978.

[15] P. Wust, M. Seebass, J. Nadobny, P. Deuflhard, G. Moenich, and R. Felix, "Simulation studies promote technological development of radiofrequency phased array hyperthermia," *Int. J. Hyperthermia*, vol. 12, no. 4, pp. 477–494, 1996.

Jacek Nadobny was born in Kalisz, Poland, in 1959. He received the M.S. and Ph.D. degrees in electrical engineering from the Technical University, Berlin, Germany, in 1987 and 1993, respectively.

He is currently a Research Engineer at the Clinic for Radiation Medicine, Charité–Campus Virchow-Klinikum, Medical School of Humboldt University at Berlin, Berlin, Germany, and also at the Konrad–Zuse–Zentrum Berlin (ZIB), Berlin, Germany, where he is engaged in the development of computer simulation for hyperthermia cancer therapy and applicator design.

Dennis Sullivan (M'89–SM'95) received the Ph.D. degree from the University of Utah, Salt Lake City, in 1987.

From 1987 to 1992, he developed treatment planning for hyperthermia cancer therapy at Stanford University. He is currently Associate Professor of electrical engineering at the University of Idaho, Idaho Falls, where his research interests are nonlinear optical simulation and quantum solid-state simulation.

Peter Wust was born in Berlin, Germany, in 1953. He received the M.S. degree (Dipl.-Phys.) in physics and the M.D. (Dr.-Med.) degree from the Free University of Berlin, Berlin, Germany, in 1978 and 1983, respectively.

Since 1984, he has been with the Department of Radiation Oncology, Charité–Campus Virchow-Klinikum, Medical School of Humboldt University at Berlin, Berlin, Germany. He received the board certification of radiation oncology in 1990, and, since 1993, has been working as an Assistant Professor and Consultant for radiation oncology. He has performed research in nuclear physics and radiation oncology. Since 1988, he has been particularly interested in the methodical and clinical aspects of hyperthermia in cancer therapy and, since 1994, he has been Coordinator of a collaborative research project on hyperthermia (Sonderforschungsbereich 273).

Martin Seebass was born in Bad Neuenahr, Germany, in 1960. He received the diploma and Ph.D. degrees in physics from the University of Heidelberg, Heidelberg, Germany, in 1983 and 1990, respectively.

From 1985 to 1991, he was with the German Cancer Research Center, Heidelberg, Germany. Since May 1991, he has been with the Konrad–Zuse–Zentrum fuer Informationstechnik Berlin (ZIB), Berlin, Germany, where he is involved with the development of computer simulation for hyperthermia cancer therapy.

Peter Deuflhard was born near Munich, Germany, in 1944. He received the physics degree from the Munich Institute of Technology, Munich, Germany, in 1968, and the Ph.D. degree in mathematics from the University of Cologne, Cologne, Germany, in 1972.

From 1978 to 1986, he was Full Professor of mathematics (with a specialty in numerical analysis) at the University of Heidelberg, Heidelberg, Germany. He then moved to Berlin, Germany, to build up the Konrad–Zuse–Zentrum fuer Informationstechnik Berlin (ZIB), Berlin, Germany, as a center of high-performance scientific computing. He is currently the Director of ZIB, and also Full Professor of scientific computing at the Free University of Berlin, Munich, Germany. His special fields of interest are differential equation modeling, efficient simulation, and optimization. He has worked in many different application areas, including space technology, chemical engineering, medicine, and electronics. His main research contributions are algorithms for the fast and reliable solution of ordinary and partial differential equation systems, which are typically large scale and originating from engineering or medicine.

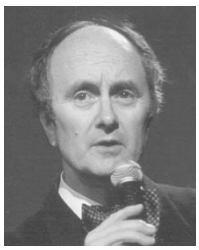

Roland Felix was born in Berlin, Germany, on May 15, 1938. He received the M.D. degree form the University of Munich, Munich, Germany, in 1962.

In 1964, he began his scientific work at Bonn University, Bonn, Germany, where his main interest was heart and pulmonary diseases, as well as cerebral microcirculation. Since 1978, he has been Full Professor of Radiology at Charité–Campus Virchow-Klinikum, Medical School of Humboldt University at Berlin, Berlin, Germany. In 1983, together with the Schering Company, he began work on the development of Gadolinium-DTPA, a new contrast agent for magnetic resonance imaging. In 1986, he set up the division of therapeutical hyperthermia and established telecommunication.